Role of nitrogen substitution in phenyl ring on excited state intramolecular proton transfer and rotamerism of 2-(2′-hydroxyphenyl)benzimidazole: A theoretical study

Francis A. S. Chipem, Nihar Dash, and G. Krishnamoorthy[a)]
Department of Chemistry, Indian Institute of Technology Guwahati, Guwahati 781 039, India

(Received 22 October 2010; accepted 14 February 2011; published online 14 March 2011)

A comparative study of 2-(2′-hydroxy-3′-pyridyl)benzimidazole (2′,3′-HPyBI), 2-(3′-hydroxy-4′-pyridyl)benzimidazole (3′,4′-HPyBI), 2-(4′-hydroxy-3′-pyridyl)benzimidazole (4′,3′-HPyBI), 2-(3′-hydroxy-2′-pyridyl)benzimidazole (3′,2′-HPyBI), and 2-(5′-hydroxy-4′-pyrimidinyl)benzimidazole (5′,4′-HPymBI) with 2-(2′-hydroxyphenyl)benzimidazole (HPBI) was performed theoretically to evaluate the effect of nitrogen substitution in the phenolic ring on the photophysics and rotamerism of HPBI. Density functional theory (DFT) and configuration interaction singles (CIS) combined with time-dependent DFT were employed for ground and excited state studies, respectively. Different possible molecular forms were considered for each molecule viz., *cis*-enol, *trans*-enol, open-enol, and keto forms. The computational results revealed that *cis*-enol is the most stable form in the ground state for all the molecules except in 2′,3′-HPyBI. In 2′,3′-HPyBI, K-2 keto is the most stable form. Water molecule assisted interconversions between different forms of 2′,3′-HPyBI were examined theoretically. Excitation and emission energies for all the forms have been calculated theoretically and the values are in good agreement with the available experimental data. The calculations show that intramolecular proton transfer (ESIPT) is endothermic in the ground state while it is exothermic in the first excited singlet state (except 5′,4′-HPymBI). The barrier for the excited state ESIPT reaction increases with nitrogen substitution. Torsional rotation between the benzimidazole and the pyridinyl/pyrimidinyl rings in the S_1 state depicts that twisted-keto structures involve charge transfer from the hydroxypyridinyl/hydoxypyrimidinyl to the benzimidazole ring. However, the formation of twisted-keto is not energetically favored in these systems. © *2011 American Institute of Physics*. [doi:10.1063/1.3562124]

I. INTRODUCTION

Proton transfer reactions are of fundamental importance in chemical and biological processes.[1,2] In particular excited state intramolecular proton transfer (ESIPT) (Refs. 3 and 4) process receives much attention due to simplicity of the phenomenon and its wide applicability in fluorescence sensing, lasers, data storage, information processing, photostabilizers, etc.[5–10] 2-(2′-Hydroxyphenyl)benzazoles form important class of molecules that undergo ESIPT. Among them 2-(2′-hydroxyphenyl)benzoxazole, 2-(2′-hydroxyphenyl)benzothiazole, 2-(2′-hydroxyphenyl)benzimidazole (HPBI), and 2-(2′-hydroxy-5′-methylphenyl) benzotriazole have been studied extensively both experimentally and theoretically.[11–17] 2-(2′-Hydroxyphenyl)benzoxazole was suggested as a phototautomerizable model DNA base pair with differential stabilization for enol and the keto tautomers in the major and minor grooves.[18,19] HPBI acts as tunable laser dye and, on the other hand, the corresponding oxazole and thiazole were examined for their potential applications in nonlinear optics and light emitting devices.[20–22] 2-(2′-Hydroxy-5′-methylphenyl)benzotriazole and related molecules are used as UV photostabilizers.[16] In addition these molecules are used as fluorescent probes for various applications.[23,24] Thus, a detailed study of these and related molecules may contribute to the improvement of their applications.

Dogra's group and Rodríguez's group have been actively studying the role of nitrogen substitution in different parts of HPBI. Since the first work on fluorescence study of HPBI by Dogra and his group,[25] those researchers have concentrated on nitrogen substitution in the benzene ring of HPBI.[26–28] Their works revealed that N-heteroatom in the benzene ring reduces the quantum yield, and the excited state lifetimes strongly depend not only on the presence of nitrogen but also on its position. Rodríguez's group[29,30] examined the role of the nitrogen substitution on the phenolic ring by studying 2-(3′-hydroxy-2′-pyridyl)benzimidazole (3′,2′-HPyBI) and they found that the quantum yield of the phototautomer increases by nitrogen substitution. However, Dogra showed that when the position of substitution changes, 2-(2′-hydroxy-3′-pyridyl)benzimidazole (2′,3′-HPyBI) does not undergo ESIPT.[31] All these results clearly suggest that the presence and position of nitrogen atom strongly perturb the ESIPT and the related photophysics of these molecules.

Recently we have examined theoretically the effect of nitrogen substitution in the benzene ring of HPBI.[32] Our investigations revealed that the feasibility of ESIPT decreases with nitrogen substitution in the benzene ring. But the

a)Electronic mail: gkrishna@iitg.ernet.in. Tel.: +91-3612582315. Fax: +91-3612582349.

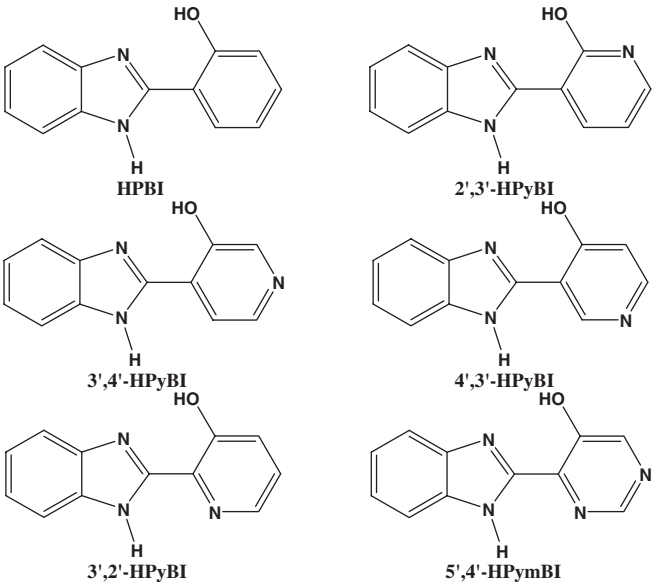

FIG. 1. HPBI and nitrogen substituted molecules.

nitrogen substitution enhances the torsional induced non-radiative process through the formation of proton coupled charge transfer twisted-keto tautomer.

Now, we have extended our studies to examine theoretically the role of nitrogen substitution in the phenolic ring of HPBI on ESIPT and rotamerism. The molecules we considered in this work are 2′,3′-HPyBI, 2-(3′-hydroxy-4′-pyridyl)benzimidazole (3′,4′-HPyBI), 2-(4′-hydroxy-3′-pyridyl)benzimidazole (4′,3′-HPyBI), 3′,2′-HPyBI, and 2-(5′-hydroxy-4′-pyrimidinyl)benzimidazole (5′,4′-HPymBI) (Fig. 1).

II. COMPUTATIONAL DETAILS

All the computations were performed with a developed version of GAUSSIAN 03W.[33] The ground state molecular geometries of each compound were obtained by full optimization of structural parameters employing Berny optimization algorithm contained within the program by density functional calculation in spin restricted shell wavefunction manner.[34,35] The hybrid functional B3LYP containing Becke's gradient corrected exchange functional containing 20% of Hartree–Fock exchange[36] and correlation functional of Lee, Yang, and Paar (LYP),[37] given by the expression

$$aE_X^{\text{Slater}} + (1-a)E_X^{\text{HF}} + b\,\Delta E_X^{\text{Becke}} + E_C^{\text{VWN}} + c\,\Delta E_C^{\text{LYP}} \quad (1)$$

was used in the calculations. The constants a, b, and c are semiempirical coefficients with values 0.8, 0.72, and 0.81, respectively. The standard 6-31G(d) was used as the basis set. Time-dependent density functional theory (TDDFT) is the uprising method for electronic structure calculations in the excited states including proton transfer reactions due to its moderate efficiency and accuracy.[38–41] However, it is reported in few cases the optimization by TDDFT method resulted in incorrect ordering of energies.[42] The geometries as well as molecular properties obtained at the configuration interaction singles (CIS) (Ref. 43) level are quite reasonable and correct, at least as a first approximation for a variety of molecules.[44,45] The TDDFT calculations over CIS optimized geometries have been proven to be an efficient approach in predicting energy parameters for various systems.[32,46–49] Moreover, TDDFT method employing B3LYP functional is shown to be reliable in treating vertical excitation energies even for charge transfer states.[50] Therefore, we have implemented the hybrid method TDDFT//CIS for energy calculations in the excited state. The excited S_1 state geometries were optimized using *ab initio* restricted configuration interaction singles RCIS/6-31G(d) approach. Solvent stabilization effects have also been studied using the integral equation formalism-polarizable continuum (IEF-PCM) model[51,52] by selecting a nonpolar solvent (cyclohexane) and a polar solvent (acetonitrile). In all the cases for optimization, the 6-31G(d) basis set was used but the molecular energies and other properties were obtained using 6-31+G(d,p) basis set. The minimum energy nature of the geometries was confirmed by vibration frequency calculations performed on the optimized stationary point geometries and first-order transition states. Vertical excitation energy calculations were performed on the optimized ground and S_1 state geometries by TDDFT/B3LYP/6-31+G(d,p) for the assignment of excitation and emission energies, respectively. The convergence threshold for the energies and residual forces on the atoms during geometry optimization (both the ground and the excited states) were 10^{-8} hartree and 4.5×10^{-4} hartree/bohr, respectively.

III. RESULTS AND DISCUSSION

A. Rotamers and tautomers

The important stationary point molecular structures for all the molecules (except 2′,3′-HPyBI) are *cis*, open, and *trans* enols and the keto form (Fig. 2). The optimized energy parameters for all these forms in the S_0 state as well as the S_1 state are compiled in Table I (Tables S1 and S2 of supplementary material) (Ref. 53) along with the transition energies for different electronic transitions. The dihedral angle between the benzimidazole and the phenyl rings is 0° in *cis*- and open-enol conformers, and is 180° in *trans*-enol conformer. The dipole

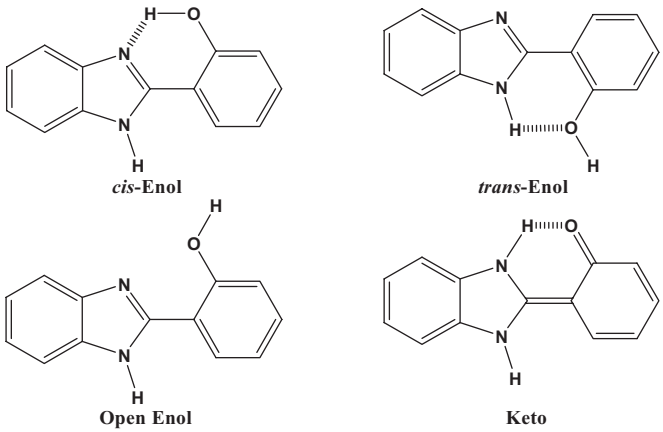

FIG. 2. Isomeric forms of HPBI.

TABLE I. Transition energies for different enols and keto form of molecules in the S_0 and S_1 states in vacuum.[a]

Parameter	*cis*-Enol	Open-enol	*trans*-Enol	Keto
		HPBI[b]		
ΔE (eV)	0.0 (0.0)[c]	0.6303 (0.6137)	0.2597 (0.2621)	0.4075 (–0.3387)
Excitation[d]	316 (293, 318, 332)[e]	311	307 (304, 326)[e]	389
Emission[d]	341	344	343 (360)[e]	429 (458)[e]
		2′,3′-HPyBI		
ΔE (eV)	0.0 (0.0)	0.3600 (0.2967)	−0.0411 (−0.1062)	0.4014 (−0.1705)
Excitation	317	321	321	379
Emission	347	354	355	406
		3′,4′-HPyBI		
ΔE (eV)	0.0 (0.0)	0.5755 (0.5669)	0.2227 (0.2243)	0.4106 (−0.3635)
Excitation	320	317	315	398
Emission	343	345	345	438
		4′,3′-HPyBI		
ΔE (eV)	0.0 (0.0)	0.6307 (0.5310)	0.3319 (0.2011)	0.3368 (−0.2991)
Excitation	299	306	307	358
Emission	332	340	343	394
		3′,2′-HPyBI		
ΔE (eV)	0.0 (0.0)	0.6075 (0.5164)	0.7257 (0.6795)	0.3682 (−0.2500)
Excitation[d]	320 (328)[f]	330	326	386
Emission[d]	347	357	353	415 (458)[f]
		5′,4′-HPymBI		
ΔE (eV)	0.0 (0.0)	0.5505 (0.4592)	0.6685 (0.5873)	0.3680 (−0.7086)
Excitation	323	337	336	439
Emission	347	354	354	490

[a]Energy difference, ΔE in eV with respect to *cis*-enol. Values in parentheses are that correspond to the S_1 state. Transition energies are in nm. All experimental data are that of molecule in dioxane.
[b]From Ref. 32 except open-enol.
[c]Energy of *cis*-enol in the S_0 and the S_1 states are −18 671.5598 eV and –18 667.5684 eV, respectively.
[d]Values in parentheses are experimental data.
[e]Reference 32.
[f]Reference 54.

moment of *trans*-enol is higher than that of *cis*-enol in all the molecules, but for 3′,4′-HPyBI and 2′,3′-HPyBI, the dipole moment of *trans*-enol is less than that of *cis*-enol. In all the molecules, *cis*-enol which forms intramolecularly hydrogen-bonded structure is the most stable geometry in the ground state. 2′,3′-HPyBI is an exception which will be discussed later. Compared to HPBI the relative stability of *cis*-enol to *trans*-enol decreases in 3′,4′-HPyBI and 2′,3′-HPyBI. However, the relative stability of *cis*-enol to *trans*-enol increases in 3′,2′-HPyBI, 5′,4′-HPymBI, and 4′,3′-HPyBI. In particular the *trans*-enol is the most unstable form of 3′,2′-HPyBI and 5′,4′-HPymBI and is due to lone pair repulsion between the imidazo nitrogen and the pyrido nitrogen. The presence of additional nitrogen reduces the repulsion in 5′,4′-HPymBI, hence the relative stability of *cis*- to *trans*-enol increases in 5′,4′-HPymBI when compared to 3′,2′-HPyBI. Except 5′,4′-HPymBI and 3′,2′-HPyBI, in all other four molecules *trans*-enol is more stable than open-enol and keto form in the ground state. The open-enols are expected to be dominant only in protic solvent.[30] Rodríguez-Prieto *et al.* showed that in nonaqueous solvents, 3′,2′-HPyBI exists only as *cis*-enol in the ground state and as keto in the excited state.[54] Their Hartree–Fock calculations of 3′,2′-HPyBI also predicted planar structure for the molecule.

The potential energy pathway for conversion of *cis*-enol to *trans*-enol for different molecules was constructed by optimizing the molecular geometries with different preset torsional angle between the two aromatic planes (Fig. 3). The

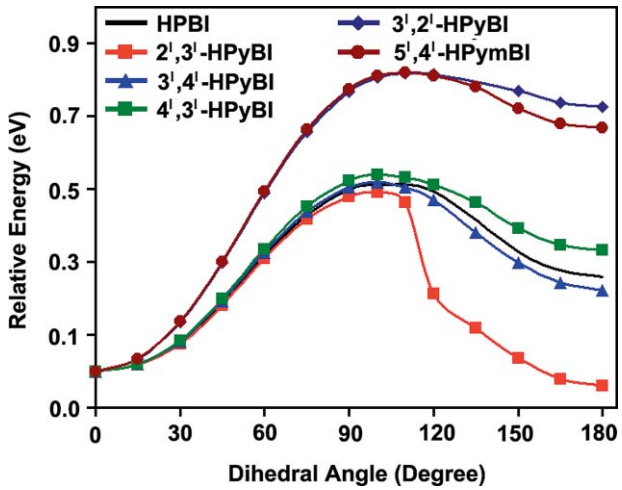

FIG. 3. Plot of molecular energy as a function of torsional angle between the two aromatic rings for different molecules in vacuum.

TABLE II. Properties of the planar and twisted keto tautomers in vacuum.

	HPBI[a]		2′,3′-HPyBI		3′,4′-HPyBI		4′,3′-HPyBI		3′,2′-HPyBI		5′,4′-HPymBI	
	Planar	Twisted	Planar	Twisted	Planar	Twisted	Planar	Twisted	Planar	Twisted	Planar[e]	Twisted
S_1 energy[b] (eV)	0.0	−0.2619	0.0	−0.1961	0.0	−0.1846	0.0	−0.0134	0.0	0.0462	0.0	0.5584
$S_1 \leftarrow S_0$ (eV)	2.89	0.75	3.05	0.90	2.83	0.85	3.15	1.34	2.99	0.93	2.53	1.09
State nature	$\pi\pi^*$	Biradicaloid	$\pi\pi^*$	Biradicaloid	$\pi\pi^*$	Biradicaloid	$\pi\pi^*$	Biradicaloid	$\pi\pi^*$	Biradicaloid	$n\pi^*$ $\pi\pi^*$	Biradicaloid
Oscillator strength	0.3300	0.0001	0.4426	0.0001	0.3279	0.0001	0.3107	0.0001	0.4494	0.0005	0.0007[e]	0.0003
						Dipole moment (D)						
S_1 state	4.92	3.62	7.84	5.04	7.17	2.46	5.31	1.22	4.02	3.33	6.55	0.68
S_0 state	5.88	8.18	8.62	9.53	8.82	10.71	7.19	9.1	4.81	7.28	7.64	9.93
						Charge on hydroxypyridine/pyrimidine moiety						
S_1 state	−0.5423	−0.0816	−0.4601	−0.0974	−0.4418	−0.0997	−0.4337	−0.1052	−0.4796	−0.1211	−0.5068	−0.1357
S_0 state	−0.8496	−0.6536	−0.2510	−0.5304	−0.8196	−0.1283	−0.5377	−0.1931	−0.4859	−0.4198	−0.5888	−0.2816
Φ_f[c]	0.22[d]								0.49[d]			

[a]Reference 32.
[b]Relative energy with respect to the planar keto.
[c]Fluorescence quantum yields (Φ_f) are that of tautomers in acetonitrile.
[d]Reference 54.
[e]The lowest excited state is $n\pi^*$ with oscillator strength 0.0007, the second excited state is $\pi\pi^*$ that has oscillator strength 0.4475.

calculations suggest that like HPBI, all these nitrogen substituted molecules can also be present in these two rotameric forms. The barrier height for the conversion increases with nitrogen substitution. Again 2′,3′-HPyBI is an exception and it has lower energy barrier than HPBI. Relative to other molecules the barrier height for conversion is nearly 1.6 times more in 5′,4′-HPymBI and 3′,2′-HPyBI, where the lone pair repulsion reduces the stability of *trans*-enol. Reduction in repulsion due to additional nitrogen in 5′,4′-HPymBI increases the barrier for the reverse process.

Photoexcited molecule from the Franck–Condon region undergoes vibration transitions to reach the relaxed geometry in the first excited state or relax to keto tautomer through ESIPT. The energies of the conformationally relaxed state for all the isomers are presented in Table I. The distance between the proton donor (oxygen atom) and the proton acceptor (nitrogen atom) in keto form increases in the S_1 state. In the first excited singlet state, as expected, the keto form is the most stable form. Though *cis*-enol is more stable than *trans*-enol, the relative stability of *trans*-enol for the nitrogen substituted molecules increases in the S_1 state relative to that in the ground state. It is just opposite to that observed in HPBI, where the relative stability of *trans*-enol decreases in the S_1 state compared to that in the ground state.

The longest wavelength transition of the enolic forms in all the molecules have $\pi\pi^*$ character. Though the keto forms of mono nitrogen substituted molecules have $\pi\pi^*$ state as the emitting state, in dinitrogen substituted 5′,4′-HPymBI the keto form has $n\pi^*$ state as the lowest excited state and $\pi\pi^*$ state as the higher excited state (Table II and Fig. 4). The excitation and emission maxima in all the isomeric forms are redshifted on nitrogen substitution. The redshifts suggest that the lone pair of electrons in the substituted nitrogen is involved in conjugation. 4′,3′-HPyBI, where the nitrogen is substituted at meta position to the electron withdrawing benzimidazole, is an exception. The spectral maxima for all the forms of 4′,3′-HPyBI are blueshifted relative to HPBI.

2′,3′-HPyBI is a special case, in the sense, it can exist in two additional keto forms (K-1 and K-2, Fig. 5). Dogra has studied the photophysics of 2′,3′-HPyBI and found that K-2 keto tautomer is the most stable form in both S_0 and S_1 states.[31] Our calculated results were consistent with his observation that K-2 form is most stable in the ground state and its stability increases further more in the excited state (Tables I and III). Interestingly *cis*-enol, the most stable form in other molecules, is less stable than *trans*-enol by

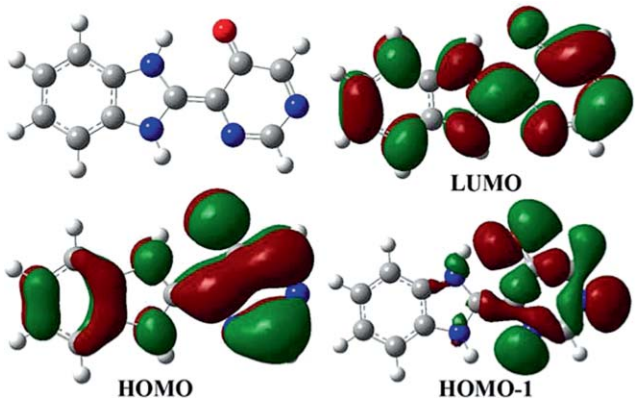

FIG. 4. Frontier molecular orbitals of the keto form of 5′,4′-HPymBI [HOMO-1-LUMO ($n\pi^*$) excited state has lower energy than HOMO-LUMO ($\pi\pi^*$) excited state].

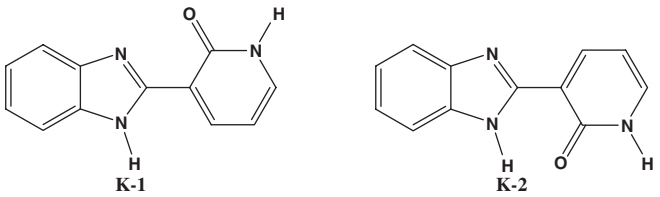

FIG. 5. Ground state keto tautomers of 2′,3′-HPyBI.

TABLE III. Important parameters of 2′,3′-HPyBI for the keto forms K-1 and K-2 in the S_0 and S_1 states (within parentheses) in vacuum.[a]

Parameter	K-1	K-2
ΔE[a] (eV)	0.3985 (–0.1024)	−0.2445 (−0.7817)
Excitation (nm)		
Theoretical	363	372
Experimental[b]	...	386
Emission (nm)		
Theoretical	400	407
Experimental[b]	...	404

[a]Energy difference in eV is with respect to *cis*-enol.
[b]Experimental data (0–0 transition) are that of molecule in dioxane (Ref. 31).

0.0411 eV. The experimental excitation and emission wavelengths for 0–0 transition of K-2 keto in dioxane are 386 and 404 nm, respectively.[31] Our present calculated values 372 and 407 nm for excitation and emission, respectively, are in better agreement with the experimental values than the theoretical values, 367 and 443 nm, respectively, reported earlier by Dogra.[31] Alike the keto tautomer formed by ESIPT, in K-2 keto the lowest energy transition is mainly described by $\pi\pi^*$, with small contribution (16%) from the local excitation of benzimidazole moiety (LE_B) to π^* (Table IV and Fig. S1).

The effect of solvent on the relative energies of different forms was studied in two limiting solvents, nonpolar cyclohexane ($\varepsilon = 2.023$) and polar acetonitrile ($\varepsilon = 36.64$) using IEF-PCM (Table V). The increase in polarity decreases the relative stability of *cis*-enol compared to other structural forms. However, in 2′,3′-HPyBI, where *trans*-enol is more stable than *cis*-enol (in vacuum), the energy difference between *trans*-enol and *cis*-enol decreases in cyclohexane; and in acetonitrile, *cis*-enol becomes more stable than *trans*-enol. The keto forms of 2′,3′-HPyBI, K-1 and K-2 also get stabilized with polarity of the medium.

B. Intramolecular proton transfer

After photoexcitation, *cis*-enol undergoes ultrafast proton transfer that results in keto tautomer.[55,56] In most of the molecules, ESIPT process is very fast and occurs in femto- to subpicosecond time scale. The potential energy surface (PES) of the intramolecular proton transfer (IPT) process in both ground and excited states was generated as a function of the distance between the dissociable hydrogen and oxygen of the phenolic hydroxyl group of *cis*-enol geometries. As the distance between the phenolic oxygen and proton gets farther away, the proton comes closer to the imidazole nitrogen, i.e., the hydrogen bond between the dissociable hydrogen and the imidazo nitrogen becomes covalent bond. After relaxation, the keto product decays to the Franck–Condon region in its ground state. In the ground state, the keto form is unstable and reverses back the proton transfer to form *cis*-enol.

TABLE IV. Properties and nature of the transition of tautomer rotamers K-1 and K-2 of 2′,3′-HPyBI in vacuum.

	K-1	K-2
$S_1 \leftarrow S_0$ (eV)	3.10	3.05
State nature	$\pi\pi^*$	$\pi\pi^*$ (84%) $LE_B\pi^*$ (16%)
Oscillator strength	0.6196	0.5033
Φ_f		0.48[a]
	Dipole moment (D)	
S_1 state	5.71	2.09
S_0 state	6.68	4.49

[a]Fluorescence quantum yield in dioxane from Ref. 31.

Though 2′,3′-HPyBI and 3′,2′-HPyBI have been examined theoretically,[31,54] complete PES for proton transfer process was not simulated for any of these nitrogen substituted molecules. The PES for different molecules are shown in Fig. 6 and the energy differences and the barrier heights are given in Table VI. In all the molecules, *cis*-enol is the stable form in the S_0 state while keto, the proton transferred product, is more stable in the S_1 state. This shows that IPT is thermodynamically not favored in the ground state but favored in the S_1 state. However, *cis*-enol form of 5′,4′-HPymBI is more stable than keto in both S_0 and S_1 states.

Contrary to nitrogen substitution in benzene ring, the relative stability of the keto form with respect to *cis*-enol decreases in the S_1 state upon nitrogen substitution in the phenolic ring. Exception is 4′,3′-HPyBI, where nitrogen is substituted at *para* position to hydroxyl group and the electron withdrawing nature of nitrogen makes it more acidic. Although in the first excited state 2′,3′-HPyBI is more stable in the keto form than *cis*-enol form, no ESIPT was reported. The absence of ESIPT in 2′,3′-HPyBI is due to the absence of *cis*-enol in the ground state which has the prerequisite intramolecular hydrogen bond that is essential for ESIPT (as mentioned earlier, K-2 keto is the most stable form).[31] Water assisted relay transfer of proton in 2′,3′-HPyBI is discussed in Sec. III C.

The energy barrier for the IPT in the S_0 state also increases upon nitrogen substitution, 4′,3′-HPyBI is an exception. In the first excited state, the barrier decreases with respect to the ground state. This is consistent with the fact that the interconversion of the enol form to the keto form is favored in the S_1 state. Unlike the S_0 state, in the S_1 state, the barrier increases in all the nitrogen substituted molecules and it is highest in dinitrogen substituted 5′,4′-HPymBI. Thus, substitution of nitrogen in the phenolic ring less favors the IPT process. The effect is just opposite to the substitution of nitrogen in the benzene ring of HPBI.[30] Despite this the opposite trend is observed in the fluorescence quantum yield of the keto form.[26–30,57] The fluorescence yield decreases when nitrogen is substituted in benzene ring and increases on substitution in the phenolic ring.

The solvent effect calculations suggest that the keto tautomer is more stabilized in the S_1 state upon increasing polarity of the solvent (Table S3). The barrier for proton transfer also decreases in acetonitrile compared to cyclohexane in both S_0 and S_1 states. On the other hand, the barrier for the reverse proton transfer in both ground and first excited states increases in polar acetonitrile, but it decreases in the S_1 state for 4′,3′-HPyBI and 5′,4′-HPymBI.

TABLE V. Relative energies in eV at S_0 and S_1 states in cyclohexane and acetonitrile.[a]

Molecule	Solvent	*cis*-Enol	Open-enol	*trans*-Enol	Tautomer	K-1	K-2
HPBI	Cyclohexane	0.0 (0.0)	0.4739 (0.5002)	0.2145 (0.2072)	0.3259 (−0.3392)		
	Acetonitrile	0.0 (0.0)	0.3179 (0.2855)	0.1260 (0.0938)	0.1748 (−0.4267)		
2′,3′-HPyBI	Cyclohexane	0.0 (0.0)	0.3159 (0.2534)	−0.0195 (−0.0703)	0.2900 (−0.2205)	0.2612 (−0.2024)	−0.2761 (−0.7372)
	Acetonitrile	0.0 (0.0)	0.1766 (0.1718)	0.0463 (−0.0259)	0.0736 (−0.3827)	−0.0628 (−0.6483)	−0.2816 (−0.9365)
3′,4′-HPyBI	Cyclohexane	0.0 (0.0)	0.4853 (0.4443)	0.1857 (0.1668)	0.3143 (−0.3874)		
	Acetonitrile	0.0 (0.0)	0.2411 (0.2402)	0.1091 (0.0604)	0.1372 (−0.4816)		
4′,3′-HPyBI	Cyclohexane	0.0 (0.0)	0.5281 (0.4372)	0.2704 (0.1581)	0.2335 (−0.2483)		
	Acetonitrile	0.0 (0.0)	0.2976 (0.2328)	0.1311 (0.0292)	0.0517 (−0.3227)		
3′,2′-HPyBI	Cyclohexane	0.0 (0.0)	0.4966 (0.4274)	0.5887 (0.5660)	0.2764 (−0.3307)		
	Acetonitrile	0.0 (0.0)	0.2526 (0.2131)	0.2775 (0.2916)	0.1206 (−0.3932)		
5′,4′-HPymBI	Cyclohexane	0.0 (0.0)	0.0164 (0.3673)	0.0199 (0.4893)	0.0095 (−0.5535)		
	Acetonitrile	0.0 (0.0)	0.0080 (0.1663)	0.0093 (0.1877)	0.0027 (−0.5564)		

[a]Values in parentheses are that of S_1 state.

C. Intermolecular proton transfer in 2′,3′-HPyBI

As reported by Dogra,[31] the absence of ESIPT in 2′,3′-HPyBI can be attributed to the nonexistence of *cis*-enol in the ground state. In the ground state the molecule is predominantly present in K-2 form, which is the *trans* conformer of K-1. Both K-1 and K-2 are keto tautomers of 2′,3′-HPyBI and are different from the one that is formed by ESIPT. This renders a special interest on the interconversion of different forms of 2′,3′-HPyBI in the ground state. In the absence of intramolecular hydrogen bond between the proton donor and the proton acceptor, the transfer should be assisted by protic solvents. We have examined water mediated conversion of open- and *trans*-enol to K-1 and K-2 tautomers, respectively, by adding a water molecule.

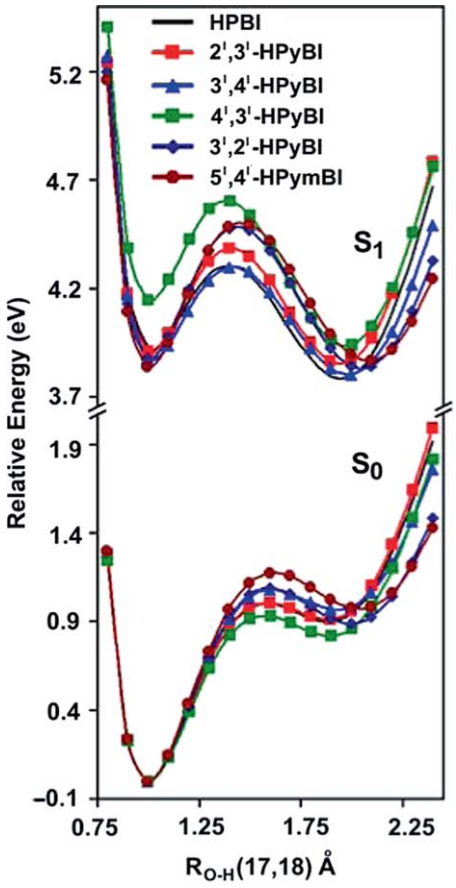

FIG. 6. Simulated potential energy surfaces for intramolecular proton transfer reaction in vacuum for different molecules.

TABLE VI. Energy difference and barrier for proton transfer reaction (eV) in vacuum.[a]

		Energy barrier	
Energy state	ΔE	*cis*-Enol	Keto-tautomer
	HPBI[b]		
S_1	−0.1326	0.3778	0.5104
S_0	0.9195	0.9986	0.0790
	2′,3′-HPyBI		
S_1	−0.0468	0.4743	0.5211
S_0	0.9100	1.0066	0.0966
	3′,4′-HPyBI		
S_1	−0.0743	0.4207	0.4950
S_0	0.9701	1.0806	0.1105
	4′,3′-HPyBI		
S_1	−0.2025	0.4596	0.6621
S_0	0.8166	0.9317	0.1151
	3′,2′-HPyBI		
S_1	−0.0346	0.6000	0.6345
S_0	0.8874	1.0896	0.2022
	5′,4′-HPymBI		
S_1	0.0297	0.6572	0.6275
S_0	0.9747	1.1734	0.1986

[a]Energy difference between *cis*-enol and keto-tautomer.
[b]Reference 32.

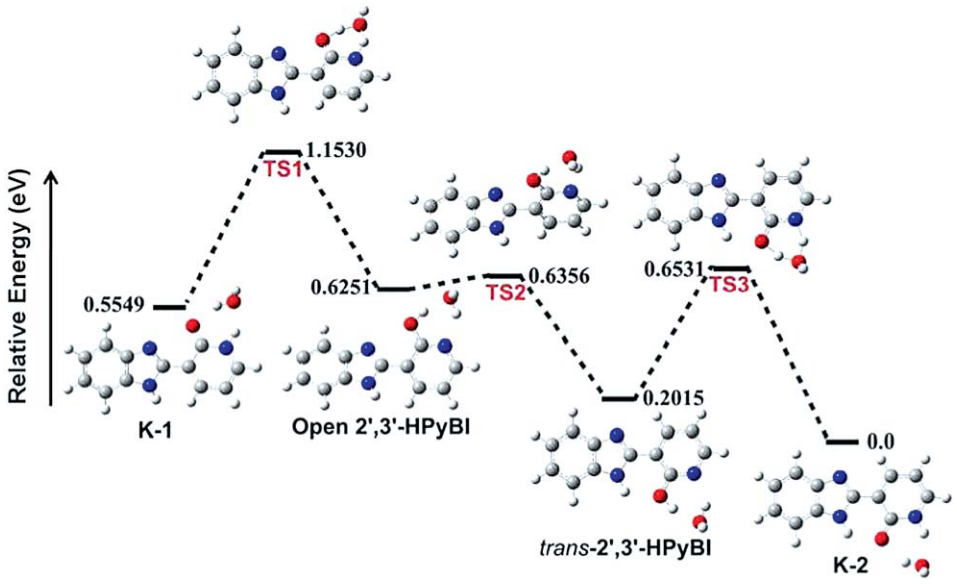

FIG. 7. Water molecule assisted proton transfer in 2′,3′-HPyBI.

In the absence of water molecule, open-enol structure is more stable than K-1 (Tables I and III). Upon addition of a water molecule K-1 becomes more stable than open-enol by 0.0703 eV. The geometry of open-enol also changes to a measurable extend mainly the dihedral angle between the two aromatic rings which was 0° in the absence of water increases to 37.4°. The activation energy for the conversion of open-enol to K-1 is 0.5278 eV in case of simultaneous double proton transfer that occurs via TS1 transition state (Fig. 7 and Fig. S2). Proton transfer can also occur by stepwise process through two more different pathways: (i) the open-enol loses its phenolic proton to solvent molecule to form a phenolate–hydronium complex, followed by proton transfer from the hydronium ion to the fluorophore to form K-1 tautomer, (ii) proton is first transferred from water molecule to pyridine nitrogen of 2′,3′-HPyBI forming a pyridinium–hydroxyl ion pair and in the next step the phenolic proton is transferred to hydroxyl ion to give K-1. The activation energies of these stepwise proton transfer processes are same and are 0.5412 eV.

The energy barrier for rotation of hydrated open-enol to *trans*-enol is 0.0121 eV and *trans*-enol is more stable than K-1 tautomer. But the K-2 tautomer is the most stable form in hydrated state also. The barrier for conversion from *trans*-enol to K-2 is also less than that of open-enol to K-1. Here the barrier for simultaneous proton transfer is 0.4617 eV (Fig. 7). On the other hand, the activation energies for stepwise proton transfer via phenolate–hydronium and pyridinium–hydroxyl ion pairs are 0.4518 and 0.4516 eV, respectively.

D. Torsional rotation of keto tautomer

Charge transfer from the phenolic moiety to the azole moiety, associated with a large amplitude torsional motion of the keto tautomer, that formed by ESIPT process, is reported as a radiationless decay in 2-(2′-hydroxyphenyl)-azoles and -benzazoles.[32,57–59] To account for the temperature dependent nonradiative decay in 2-(2′-hydroxyphenyl)benzothiazole, Potter *et al.* proposed an intramolecular charge transfer in *syn*-keto tautomer in the excited state that induces the conformational motion which leads to a nonemissive twisted state.[58] Theoretical calculations on 2-(2′-hydroxyphenyl)-oxazole, -thiazole, and -triazoles also predict a charge transfer of almost full electron from the phenol portion to the azole portion, associated with high-amplitude interannular bond rotation.[17,59] Our theoretical study on HPBI and related molecules also suggested that torsional relaxation of the keto tautomer to a twisted state competes with radiative transitions and it results in fluorescence quenching.[32]

Based on the experimental work, Vázquez *et al.* proposed that the excited-state intramolecular coupled proton and charge transfer lead to a nonfluorescent intermediate in 2-(2′-hydroxyphenyl)benzazoles and 3′,2′-HPyBI.[57] It was also suggested that the relative efficiency of this radiationless decay is less favored in 3′,2′-HPyBI compared to 2-(2′-hydroxyphenyl)benzazoles. We have optimized the geometry of twisted keto in the S_1 state. As shown in Fig. 8, the increase in the electron density of the five membered ring leads to its pyramidalization, borne out by the angle ∼67° and 150° (in the S_1 state) deviation from ∼90° and 180° (Table S4 in supplementary material). Same behavior of pyramidalization with increase in electron density on the azole rings was reported for HPBI and 2-(2′-hydroxyphenyl)-oxazole and -thiazole.[32,59] The energies obtained from the present TDDFT calculations predict that like HPBI,[32] the twisted keto is more stable than planar keto in 2′,3′-HPyBI, 3′,4′-HPyBI, and 4′,3′-HPyBI (Fig. S4). But twisted keto of 3′,2′-HPyBI and 5′,4′-HPymBI are less stable than corresponding planar conformer in the S_1 state (Table II).

The present results depict a different scenario from the earlier one,[32] where the benzene ring of benzimidazole moiety in HPBI is substituted by nitrogen. In the earlier work, the twisted keto form is more stable than the planar one in all the molecules and the relative stability increases with nitrogen substitution.[32] The energy difference between the S_0 and

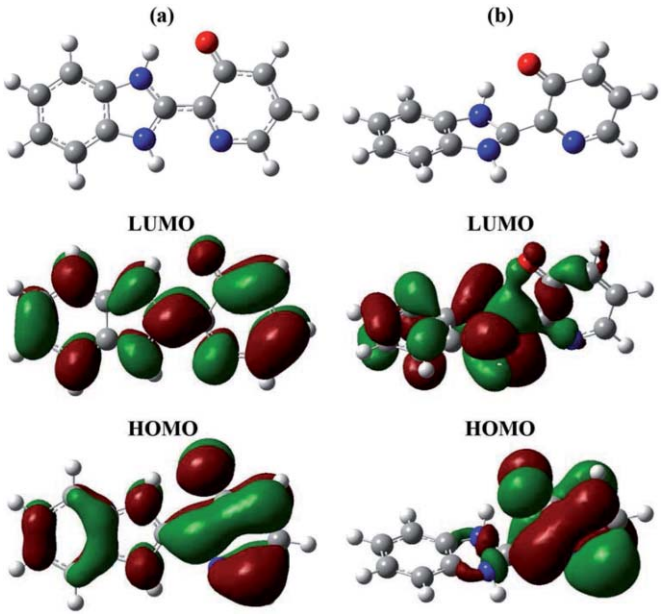

FIG. 8. Optimized structures of (a) planar keto and (b) twisted keto on the excited state surface along with corresponding frontier molecular orbitals for 3′,2′-HPyBI.

S_1 states at the twisted geometry decreases with nitrogen substitution. This provides a route for nonradiative deactivation to the ground state from the S_1 state. Thus, the radiationless decay involves large-angle motion of the excited tautomer associated with intramolecular charge transfer from the deprotonated phenol to the protonated benzimidazole ring to form the twisted keto. The efficiency of the process is related to the strength of the electron donor (dissociated phenol moiety) and electron acceptor (protonated azole). Therefore, substitution of nitrogen in the benzimidazole ring favored the formation of twisted structure. In the present case, due to incorporation of more electronegative nitrogen in the phenolic ring, the charge donating capacity of the dissociated pyridinol or pyrimidinol moiety is less than the dissociated phenol. Hence, the charge transfer is less in the present systems and thus the twisted keto tautomer is less stabilized. Contrary to nitrogen effect on benzene ring, the S_1–S_0 energy gap for the twisted keto also increases by nitrogen on phenolic moiety (Table II and Fig. S4 of supplementary material). The energy gap further increases in solvents (Table S5). Hence, it is clear that the nonradiative deactivation through the twisted keto is less important in the present system. The result is consistent with the observed higher quantum yield for 3′,2′-HPyBI ($\Phi_f = 0.49$ in acetonitrile) compared to HPBI ($\Phi_f = 0.22$ in acetonitrile).[57] It may also be noted that the fluorescence quantum yield of 2-(2′-hydroxyphenyl)benzoxazole strongly depends on temperature and viscosity. On the other hand, the fluorescence quantum yield of corresponding hydroxypyridinyl analog, whose electron donating capacity decreases due to nitrogen substitution, is independent of temperature and viscosity.[57] Thus, it may be concluded that the decrease in the nonradiative rate due to the formation of twisted keto is responsible for the different dependence on viscosity and temperature between 2-(2′-hydroxyphenyl)benzoxazole.

IV. CONCLUSION

Studies on the role of nitrogen substitution in phenolic ring of HPBI were performed theoretically. The theoretical calculations for the excitation and the emission energies are in good agreement with available literature data. The calculations show that *cis*-enol is the most stable geometry in the S_0 state in all the molecules except in 2′,3′-HPyBI where K-2 keto is the most stable form. In 2′,3′-HPyBI *trans*-enol is also more stable than *cis*-enol. The energy barrier predicted for water molecule assisted interconversion of *trans*-enol to K-2 form is lower than that of open-enol to K-1. In all the molecules except 5′,4′-HPymBI, the ESIPT process is favored in the S_1 state thermodynamically, but the energy barrier increased in nitrogen substituted molecules. The energy difference between the enol form and the keto form along the proton transfer coordinate in the S_1 state decreases with nitrogen substitution except 4′,3′-HPyBI. The calculations suggest that the nonradiative decay through torsion rotation of the excited keto tautomer to twisted structure is less important in these molecules. This is consistent with the experimental fact that the quantum yield of 3′,2′-HPyBI is higher than that of HPBI.

ACKNOWLEDGMENTS

Dedicated to Professor S. K. Dogra on the occasion of his 69th birthday.

The authors thank Department of Science and Technology, India for the funding. F.A.S.C. acknowledges CSIR, India for the Fellowship. The authors thank the reviewers for their valuable suggestions for improving the quality of the manuscript.

[1] K. Faxén, G. Gilderson, P. Ädelroth, and P. Brzezinski, Nature (London) **437**, 286 (2005).
[2] A. Douhal, S. K. Kim, and A. H. Zewail, Nature (London) **378**, 260 (1995).
[3] M. Kasha, J. Chem. Soc., Faraday Trans. 2 **82**, 2379 (1986).
[4] S. J. Formosinho and L. G. Arnaut, J. Photochem. Photobiol., A **75**, 21 (1993).
[5] Y. Wu, X. Peng, J. Fan, S. Gao, M. Tian, J. Zhao, and S. Sun, J. Org. Chem. **72**, 62 (2007).
[6] M. S. Celej, W. Caarls, A. P. Demchenko, and T. M. Jovin, Biochemistry **48**, 7465 (2009).
[7] P. Chou, D. McMorrow, T. J. Aartsma, and M. Kasha, J. Phys. Chem. **88**, 4596 (1984).
[8] G. Zhang, H. Wang, Y. Yu, F. Xiong, G. Tang, and W. Chen, Appl. Phys. B **76**, 677 (2003).
[9] S. Kumar, V. Luxami, R. Saini, and D. Kaur, Chem. Commun. (Cambridge) 2009, 3044.
[10] M. J. Paterson, M. A. Robb, L. Blancafort, and A. D. DeBellis, J. Phys. Chem. A **109**, 7527 (2005).
[11] A. Ohshima, A. Momotake, R. Nagahata, and T. Arai, J. Phys. Chem. A **109**, 9731 (2005).
[12] R. Vivie-Riedle, V. De Vaele, L. Kurtz, and E. Riedle, J. Phys. Chem. A **107**, 10591 (2003).
[13] M. Mosquera, J. C. Penedo, M. C. R. Ríos Rodríguez, and F. Rodríguez-Prieto, J. Phys. Chem. **100**, 5398 (1996).
[14] A. Pla-Dalmau, J. Org. Chem. **60**, 5468 (1995).
[15] P. Purkayastha and N. Chattopadhyay, Phys. Chem. Chem. Phys. **2**, 203 (2000).
[16] H. E. A. Kramer, in *Photochromism: Molecules and Systems*, 1st ed., edited by H. Dürr and H. Bouas-Laurent (Elsevier, Amsterdam, 1990), Chap. 16, pp. 645–684.

[17]M. J. Paterson, M. A. Robb, L. Blancafort, and A. D. DeBellis, J. Am. Chem. Soc. **126**, 2912 (2004).
[18]A. K. Ogawa, O. K. Abou-Zied, V. Tsui, R. Jimenez, D. A. Case, and F. E. Romesberg, J. Am. Chem. Soc. **122**, 9917 (2000).
[19]F. Y. Dupradeau, D. A. Case, C. Yu, R. Jimenez, and F. E. Romesberg, J. Am. Chem. Soc. **127**, 15612 (2005).
[20]C. E. Fellows, E. Täuber, C. C. Rodegheri, C. E. M. Carvalho, D. F. Acevedo, S. G. Bertolotti, and C. Barbero, Opt. Mater. **27**, 499 (2004).
[21]S. Hillebrand, M. Segala, T. Buckup, R. R. B. Correia, F. Horowitz, and V. Stefani, Chem. Phys. **273**, 1 (2001).
[22]S. M. Chang, K. L. Hsueh, B. K. Huang, J. H. Wu, C. C. Liao, and K. C. Lin, Surf. Coat. Technol. **200**, 3278 (2006).
[23]S. K. Das and S. K. Dogra, J. Chem. Soc., Faraday Trans. **94**, 139 (1998).
[24]T.-I. Kim, H. J. Kang, G. Han, S. J. Chung, and Y. Kim, Chem. Commun. (Cambridge) 2009, 5895.
[25]H. K. Sinha and S. K. Dogra, Chem. Phys. **102**, 337 (1986).
[26]M. M. Balamurali and S. K. Dogra, J. Photochem. Photobiol., A **154**, 81 (2002).
[27]G. Krishnamoorthy and S. K. Dogra, J. Lumin. **92**, 91 (2001).
[28]G. Krishnamoorthy and S. K. Dogra, J. Lumin. **92**, 103 (2001).
[29]M. Mosquera, M. C. R. Rodríguez, and F. Rodríguez-Prieto, J. Phys. Chem. A **101**, 2766 (1997).
[30]M. C. R. Rodríguez, M. Mosquera, and F. Rodríguez-Prieto, J. Phys. Chem. A **105**, 10249 (2001).
[31]S. K. Dogra, J. Mol. Struct. **734**, 51 (2005).
[32]F. A. S. Chipem and G. Krishnamoorthy, J. Phys. Chem. A **113**, 12063 (2009).
[33]M. J. Frisch, G. W. Trucks, H. B. Schlegel, G. E. Scuseria, M. A. Robb, J. R. Cheeseman, J. A. Montgomery, T. Vreven, Jr., K. N. Kudin, J. C. Burant, J. M. Millam, S. S. Iyengar, J. Tomasi, V. Barone, B. Mennucci, M. Cossi, G. Scalmani, N. Rega, G. A. Petersson, H. Nakatsuji, M. Hada, M. Ehara, K. Toyota, R. Fukuda, J. Hasegawa, M. Ishida, T. Nakajima, Y. Honda, O. Kitao, H. Nakai, M. Klene, X. Li, J. E. Knox, H. P. Hratchian, J. B. Cross, V. Bakken, C. Adamo, J. Jaramillo, R. Gomperts, R. E. Stratmann, O. Yazyev, A. J. Austin, R. Cammi, C. Pomelli, J. W. Ochterski, P. Y. Ayala, K. Morokuma, G. A. Voth, P. Salvador, J. J. Dannenberg, V. G. Zakrzewski, S. Dapprich, A. D. Daniels, M. C. Strain, O. Farkas, D. K. Malick, A. D. Rabuck, K. Raghavachari, J. B. Foresman, J. V. Ortiz, Q. Cui, A. G. Baboul, S. Clifford, J. Cioslowski, B. B. Stefanov, G. Liu, A. Liashenko, P. Piskorz, I. Komaromi, R. L. Martin, D. J. Fox, T. Keith, M. A. Al-Laham, C. Y. Peng, A. Nanayakkara, M. Challacombe, P. M. W. Gill, B. Johnson, W. Chen, M. W. Wong, C. Gonzalez, and J. A. Pople, GAUSSIAN 03, Revision E.01, Gaussian, Inc., Wallingford, CT, 2004.
[34]P. Hohenberg and W. Kohn, Phys. Rev. **136**, B864 (1964).
[35]W. Kohn and L. J. Sham, Phys. Rev. **140**, A1133 (1965).
[36]A. D. Becke, J. Chem. Phys. **98**, 5648 (1993).
[37]C. Lee, W. Yang, and R. G. Parr, Phys. Rev. B **37**, 785 (1988).
[38]M. E. Casida, in *Recent Advances in Density Functional Methods, Part I*, edited by D. P. Chong (World Scientific, Singapore, 1995), Chap. 5, pp. 155–192.
[39]E. Gross, J. Dobson, and M. Petersilka, Top. Curr. Chem. **181**, 81 (1996).
[40]G.-J. Zhao and K.-L. Han, J. Phys. Chem. A **113**, 14329 (2009).
[41]R. Casadesús, M. Moreno, and J. M. Lluch, J. Photochem. Photobiol., A **173**, 365 (2005).
[42]Z. Yang, S. Yang, and J. Zhang, J. Phys. Chem. A **111**, 6354 (2007).
[43]J. B. Foresman, M. Head-Gordon, J. A. Pople, and M. J. Frisch, J. Phys. Chem. **96**, 135 (1992).
[44]J. F. Stanton, J. Gauss, N. Ishikawa, and M. Head-Gordon, J. Chem. Phys. **103**, 4160 (1995).
[45]K. B. Wiberg, Y.-G. Wang, A. E. de Oliveira, S. A. Perera, and P. H. Vaccaro, J. Phys. Chem. A **109**, 466 (2005).
[46]M. K. Shukla and J. Leszczynski, Int. J. Quantum Chem. **105**, 387 (2005).
[47]G. Gahungu and J. Zhang, J. Phys. Chem. B **109**, 17762 (2005).
[48]M. Belletête, N. Blouin, P.-L. T. Boudreault, M. Leclerc, and G. Durocher, J. Phys. Chem. A **110**, 13696 (2006).
[49]F. A. S. Chipem, S. Chatterjee, and G. Krishnamoorthy, J. Photochem. Photobiol., A **214**, 121 (2010).
[50]C. Jamorski, J. B. Foresman, C. Thilgen, and H.-P. Lüthi, J. Chem. Phys. **116**, 8761 (2002).
[51]S. Miertuš, E. Scrocco, and J. Tomasi, Chem. Phys. **55**, 117 (1981).
[52]E. Cancès, B. Mennucci, and J. Tomasi, J. Chem. Phys. **107**, 3032 (1997).
[53]See supplementary material at http://dx.doi.org/10.1063/1.3562124 for the additional tables related to structural parameters of optimized geometries as well as their corresponding dipole moments and solvent effects on intramolecular proton transfer and S1–S0 energy gap of twisted keto. Reaction scheme on water assisted intermolecular proton transfer and potential energy surface for torsional rotation of keto tautomers are also provided.
[54]F. Rodríguez-Prieto, M. C. R. Rodríguez, M. M. González, and M. A. R. Fernández, J. Phys. Chem. **98**, 8666 (1994).
[55]S. Lochbrunner, A. J. Wurzer, and E. Riedle, J. Phys. Chem. A **107**, 10580 (2003).
[56]A. Migani, L. Blancafort, M. A. Robb, and A. D. DeBellis, J. Am. Chem. Soc. **130**, 6932 (2008).
[57]S. R. Vázquez, C. R. Rodríguez, M. Mosquera, and F. Rodríguez-Prieto, J. Phys. Chem. A **111**, 1814 (2007).
[58]C. A. Potter, R. G. Brown, F. Vollmer, and W. Rettig, J. Chem. Soc., Faraday Trans. **90**, 59 (1994).
[59]D. LeGourriérec, V. Kharlanov, R. G. Brown, and W. Rettig, J. Photochem. Photobiol., A **130**, 101 (2000).